ELSEVIER

Journal of Alloys and Compounds 239 (1996) 1–7

Journal of ALLOYS AND COMPOUNDS

Quaternary chalcogenides of the IVa metals with layered structures: 1. Preparation and structural characterization of $Tl_2Cu_2Hf_3Se_8$, $Tl_2Cu_2Zr_3S_8$ and $Tl_2Cu_2Zr_3Se_8$

Kurt O. Klepp, Doris Gurtner

Dept. Inorganic Chemistry, Kepler University, Altenbergerstr. 69, A-4040 Linz, Austria

Received 8 August 1995

Abstract

$Tl_2Cu_2Zr_3S_8$, $Tl_2Cu_2Zr_3Se_8$ and $Tl_2Cu_2Hf_3Se_8$ were prepared by reacting stoichiometric mixtures of thallium chalcogenides, copper, the IVa metal and its corresponding chalcogen at 800 °C. The compounds crystallize with a new structure type, *mC*30, space group *C*2/*m* (No. 12), $Z = 2$, with $a = 14.328(2)$ Å, $b = 3.7870(8)$ Å, $c = 14.250(2)$ Å, $\beta = 113.59(2)°$ ($Tl_2Cu_2Hf_3Se_8$); $a = 14.033(2)$ Å, $b = 3.7008(6)$ Å, $c = 13.874(3)$ Å, $\beta = 113.93(1)°$ ($Tl_2Cu_2Zr_3S_8$) and $a = 14.392(3)$ Å, $b = 3.828(1)$ Å, $c = 14.387(3)$ Å, $\beta = 113.69(2)°$ ($Tl_2Cu_2Zr_3Se_8$). The crystal structure of $Tl_2Cu_2Hf_3Se_8$ was determined from single crystal diffractometer data and refined to a conventional R value of 0.032 (717 F_o values, 48 variables). The probable isotopy of the zirconium chalcogenides was established from their powder diffraction diagrams. The characteristic feature of this new crystal structure is the formation of anionic layers $^2_\infty$-$[Cu_2Hf_3Se_8]^{2-}$ which are separated by Tl^+ ions. The layers are built up by a corrugated network of edge- and corner-sharing $HfSe_6$ octahedra with copper atoms occupying distorted tetrahedral niches. The Tl^+ ions are in a bicapped trigonal prismatic coordination through Se. The crystal structure is related to that of $KCuZrS_3$.

Keywords: Crystal structure; Sulfides; Selenides; Zirconium; Hafnium; Thallium; Copper

1. Introduction

A number of new quaternary thio- and selenozirconates $ACuZrO_3$ with copper and alkali metals have recently been found and structurally characterized by Ibers and coworkers [1,2]. Though their layered anions are built up by essentially identical building elements, distorted CuQ_4 tetrahedra and ZrQ_6 octahedra, the variability in the combination of these moieties leads to different geometries. While the anions of $KCuZrS_3$ are based on a $^2_\infty$-arrangement of edge- and corner-sharing ZrS_6 octahedra with tetrahedral niches hosting the copper atoms, the crystal structure of $NaCuZrSe_3$ contains double chains of edge-sharing octahedra which are linked together via the coinage metal atoms. Apparently the geometry of the anionic layers is in a sensitive way determined by the size relations of its constituent atoms and their cationic counterparts.

Recently we have described the novel phases $TlCuT^{IV}Q_3$ (T = Zr, Hf; Q = S, Se) which were found during an investigation of the corresponding quaternary systems [3]. These compounds crystallize in the $KCuZrS_3$ structure type which, as can be demonstrated, can be regarded as a filled variant of the Re_3B structure type.

The continuation of this study has led to the new intermediate phases $Tl_2Cu_2Zr_3S_8$, $Tl_2Cu_2Zr_3Se_8$ and $Tl_2Cu_2Hf_3Se_8$. According to their powder diffraction diagrams these compounds form an isostructural series. The crystal structure which was solved and refined for the hafnium compound fits nicely with the structural principles sketched above and will be presented in the following.

2. Experimental

Single crystals of $Tl_2Cu_2Hf_3Se_8$ were obtained as a minority phase in copper rich samples of the pseudobinary section $Tl_{2-x}Cu_xHf_2Se_6$. After the stoichiometry had been established by successful determination of the crystal structure, samples of nominal composition $Tl_2Cu_2Hf_3Se_8$, $Tl_2Cu_2Zr_3Se_8$ and $Tl_2Cu_2Zr_3S_8$ were prepared by reacting stoichiometric amounts of

PII S0925-8388(96)2263-3

TlSe or Tl_2S with the corresponding elements (99.9% purity). The powdered mixtures, sealed in silica ampoules under 10^{-2} Pa, were gradually brought to 800 °C, held at this temperature for five days and finally allowed to cool to ambient temperature at a controlled rate of 2 °C h^{-1}.

The reaction products obtained in this way were of homogeneous appearance. They were found to consist of agglomerations of intergrown microcrystalline needles showing metallic luster. Individual specimens were difficult to isolate, since the crystals were mechanically fragile and easily bent. For this reason the two zirconium compounds could only be characterized by their powder diffraction diagrams. These were obtained by the Guinier flat sample technique (quartz monochromated Cu Kα_1-radiation, $\lambda = 1.54076$ Å) using 5N Si powder ($a_o = 5.4301$ Å) as internal standard. By comparison with theoretical diffraction patterns, calculated with FINAX [4], it could be confirmed that single phase products had been obtained in the case of both selenide samples. On the Guinier film of $Tl_2Cu_2Zr_3S_8$, however, a few very weak diffraction lines were observable, which could not be attributed to the new structure type or any known phases in this system. However, these lines vanished after reannealing of the sample at 750 °C, indicating that the presumed stoichiometry was correct. Attempts to prepare the corresponding thiohafnate, $Tl_2Cu_2Hf_3S_8$, were unsuccessful. The powder diagram of a sample with this nominal composition could be interpreted as a superposition of the diagrams of $TlCuHfS_3$ [3] and HfS_2 [5]. In view of the close crystal chemical similarity of Zr and Hf these findings appear rather unexpected.

For the reasons mentioned above, the crystal structure was determined for $Tl_2Cu_2Hf_3Se_8$. Preliminary crystallographic investigations, performed using Weissenberg techniques, revealed Laue symmetry $2/m$. The only systematic extinctions were hkl: $h + k \neq 2n$, leading to $C2$, Cm and $C2/m$ as possible space groups; the last finally being adopted during the determination of the crystal structure. Several crystals had to be investigated in order to find a specimen showing sharp reflections on the Weissenberg photographs. Finally, a crystal with dimensions $0.125 \times 0.040 \times 0.025$ mm^3 was selected and mounted on a four-circle diffractometer (Enraf-Nonius CAD-4) operated with graphite monochromated Mo Kα radiation ($\lambda = 0.7107$ Å). Intensity data were collected over one quadrant of the sphere of reflection in the angular range $2 \leq 2\theta \leq 54°$ using ω–2θ scans with a theta dependent scan width of $0.90° + 0.35° \tan\theta$ (maximum scan time 180 s, background-peak-background scan mode). The evaluation of the intensities of three periodically determined control reflections indicated good crystal and electronic stability. For the determination of reliable lattice constants, 24 high angle reflections ($36° \leq 2\theta \leq 42°$) were finally selected and carefully centered on the goniometer. Refinement of their angular positions led to the lattice constants given in Table 1.

After the usual background, Lorentz and polarization corrections, symmetry equivalent reflections were averaged yielding a unique data set of 717 reflections with $|F_o| > 3\sigma(F_o^2)$. The crystal structure was solved by direct methods (MULTAN 88 [6]) in the centrosymmetric space group $C2/m$, which had been indicated by the statistics of the normalized structure factors. An E-synthesis based on $192E > 1.22$ (3176 triplet relations) revealed all atomic positions. Least-squares refinements with isotropic temperature factors rapidly converged to an R- value of 0.044. Taking into account anisotropic atomic displacements and isotropic secondary extinction led to the final R factor of 0.032 ($R_w = 0.035$). A subsequent difference Fourier synthesis revealed no physically significant peaks.

The calculations were performed on a DEC-μVAX 3520 computer using programs of the MolEN [7] crystallographic software package. Scattering factors for neutral atoms and anomalous dispersion coefficients were taken from the *International Tables for X-ray Crystallography* [8,9]. Absorption effects were accounted for by an empirical correction [10]. Further details on the structure refinement are given in Table 1. Positional parameters and anisotropic temperature factors are listed in Tables 2 and 3. A list of interatomic distances and bond angles is given in Table 4. The evaluations of the powder diagrams of $Tl_2Cu_2Zr_3S_8$ and $Tl_2Cu_2Zr_3Se_8$ are given in Tables 5 and 6 respectively.

Table 1
Crystallographic data for $Tl_2Cu_2Hf_3Se_8$

Pearson symbol:	$mC30$	
a	=	14.328(2) Å
b	=	3.7870(8) Å
c	=	14.250(2) Å
β	=	113.59(3)°
Space group:	$C2/m$ (No. 12)	
Z	=	2
V	=	708.6(Å^3)
d_x	=	7.99(g cm^{-3})
M_r	=	1702.97
$\mu_{(\mathrm{Mo\,K}\alpha)}$	=	678.62(cm^{-1})
$F(000)$	=	1416
Structure refinement		
Unique reflections		894
Observed reflections		$717 \geq 3.0\,\sigma(F_o)^2$
Variables		48
$R = \sum \lvert\lvert F_o\rvert - \lvert F_c\rvert\rvert / \sum \lvert F_o\rvert$		0.032
$R_w = \left[\sum w\lvert\lvert F_o\rvert - \lvert F_c\rvert\rvert^2 / \sum w\lvert F_o\rvert^2\right]^{1/2}$		0.035
$w = [\sigma(F_o^2)^2 + (0.005F_o^2)^2]^{-1/2}$		
residual electron density		3.28(e Å^{-3})

Table 2
Positional and thermal parameters for $Tl_2Cu_2Hf_3Se_8$

Atom	x	y	z	B_{eq} [a]
Tl	0.32809(7)	0.000	0.19605(7)	2.07(2)
Hf(1)	0.500	0.000	0.000	0.79(2)
Hf(2)	0.34575(6)	0.000	0.61897(6)	0.70(2)
Cu	0.0379(2)	0.000	0.1978(2)	1.14(5)
Se(1)	0.2983(1)	0.000	0.4177(1)	0.47(4)
Se(2)	0.0170(1)	0.000	0.3578(1)	0.66(4)
Se(3)	0.1112(1)	0.000	0.9612(1)	0.53(3)
Se(4)	0.3566(1)	0.000	0.8089(1)	0.60(4)

[a] $B_{eq} = \frac{8\pi^2}{3} \sum_i \sum_j U_{ij} a_i^* a_j^* a_i a_j$.

Table 3
Anisotropic thermal parameters ($Å^2$) for $Tl_2Cu_2Hf_3Se_8$

Atom	U_{11}	U_{22}	U_{33}	U_{12}	U_{13}	U_{23}
Tl	0.0238(4)	0.244(5)	0.0346(4)	0	0.0161(3)	0
Hf(1)	0.0099(4)	0.0093(6)	0.0097(4)	0	0.0029(3)	0
Hf(2)	0.0097(3)	0.0082(4)	0.0077(3)	0	0.0025(2)	0
Cu	0.014(1)	0.016(1)	0.011(1)	0	0.0023(8)	0
Se(1)	0.0060(7)	0.0064(9)	0.0047(7)	0	0.0012(5)	0
Se(2)	0.0076(7)	0.0071(9)	0.0102(7)	0	0.0033(5)	0
Se(3)	0.0069(7)	0.0077(9)	0.0067(7)	0	0.0040(5)	0
Se(4)	0.0083(7)	0.009(1)	0.0044(7)	0	0.0010(5)	0

The form of the anisotropic displacement parameter is $\exp \times [-2\pi^2\{h^2a^{*2}U_{11} + k^2b^{*2}U_{22} + l^2c^{*2}U_{33} + 2hka^*b^*U_{12} + 2hla^*c^*U_{13} + 2klb^*c^*U_{23}\}]$ where a^*b^* and c^* are reciprocal lattice constants.

Calculated and observed structure factors have been deposited with the Fachinformationszentrum Karlsruhe, Eggenstein Leopoldshafen, D-76344 Karlsruhe under CSD No. 59000.

3. Discussion

The selenohafnate $Tl_2Cu_2Hf_3Se_8$ crystallizes with a new structure type which is characterized by infinite layered complex anions which are parallel to $(20\bar{1})$ and are separated from each other by Tl^+ cations (Figs. 1 and 2(a)). The slightly undulated layers are based on two different selenohafnate chains running along [010]. Both chains are built up by edge-sharing $HfSe_6$ octahedra: A single trans-octahedral chain, $^1_\infty$-$[HfSe_{6/2}]$, and a double octahedral chain, $^1_\infty$-$[HfSe_{3/3}Se_{3/2}]$, are alternatingly connected with each other through common vertices to build up an infinite layer, $^2_\infty$-$[Hf_3Se_8]$. The corrugation of this octahedral layer leads to the formation of distorted tetrahedral chalcogen sites which host the copper atoms. As can be seen from Fig. 2(b) the construction pattern of the complex anions is closely related to that of $TlCuHfSe_3$ [3] ($KCuZrS_3$-type [1]) apart from the fact that only trans-octahedral chains are here involved in the formation of the Hf–Se partial structure.

As in $TlCuHfSe_3$ the thallium atoms are in a

Table 4
Interatomic distances (Å) and bond angles (°) for $Tl_2Cu_2Hf_3Se_8$

Tl–Tl	3.787(1) × 2
Tl–Cu	3.544(3) × 2
Tl–Se(1)	3.352(2)
Tl–Se(2)	3.351(2) × 2
Tl–Se(3)	3.540(2)
Tl–Se(3)	3.304(2) × 2
Tl–Se(4)	3.231(2) × 2
Hf(1)–Hf(1)	3.787(1) × 2
Hf(1)–Cu	3.256(2) × 4
Hf(1)–Se(3)	2.672(1) × 4
Hf(1)–Se(4)	2.675(2) × 2
Se(3)–Hf(1)–Se(3)	90.3(1) × 2
Se(3)–Hf(1)–Se(3)	89.7(1) × 2
Se(3)–Hf(1)–Se(3)	180.0 × 3
Se(3)–Hf(1)–Se(4)	93.9(1) × 4
Se(3)–Hf(1)–Se(4)	86.1(1) × 2
Hf(2)–Hf(2)	3.787(1) × 2
Hf(2)–Cu	3.114(2) × 2
Hf(2)–Se(1)	2.670(2)
Hf(2)–Se(1)	2.694(2) × 2
Hf(2)–Se(2)	2.654(2) × 2
Hf(2)–Se(4)	2.649(2)
Se(1)–Hf(2)–Se(4)	85.7(1) × 2
Se(1)–Hf(2)–Se(1)	86.9(1) × 2
Se(1)–Hf(2)–Se(1)	89.3(1)
Se(1)–Hf(2)–Se(2)	89.5(1) × 2
Se(1)–Hf(2)–Se(2)	89.7(1) × 2
Se(2)–Hf(2)–Se(2)	91.0(1)
Se(2)–Hf(2)–Se(4)	97.8(1) × 2
Se(1)–Hf(2)–Se(4)	169.6(1)
Se(1)–Hf(2)–Se(2)	176.3(1) × 2
Cu–Cu	3.787(1) × 2
Cu–Se(1)	3.792(3)
Cu–Se(2)	2.414(3)
Cu–Se(3)	2.413(3)
Cu–Se(4)	2.449(2) × 2
Se(4)–Cu–Se(4)	101.3(1)
Se(3)–Cu–Se(4)	107.0(1) × 2
Se(2)–Cu–Se(4)	110.4(1) × 2
Se(2)–Cu–Se(3)	119.2(1)
Se(1)–Se(4)	3.634(2) × 2
Se(1)–Se(1)	3.688(3) × 2
Se(1)–Se(2)	3.748(2) × 2
Se(1)–Se(2)	3.772(3)
Se(1)–Se(1)	3.787(1) × 2
Hf(2)–Se(1)–Hf(2)	93.1(1) × 2
Hf(2)–Se(1)–Hf(2)	89.3(1)
Se(2)–Se(2)	3.787(1) × 2
Hf(2)–Se(2)–Hf(2)	91.0(1)
Hf(2)–Se(2)–Cu	75.7(1) × 2
Se(3)–Se(4)	3.650(2) × 2
Se(3)–Se(3)	3.769(4)
Se(3)–Se(3)	3.787(1) × 2
Hf(1)–Se(3)–Hf(1)	90.3(1)
Hf(1)–Se(3)–Cu	79.5(1) × 2
Se(4)–Se(4)	3.787(1) × 2
Hf(1)–Se(4)–Hf(2)	138.3(1)
Hf(1)–Se(4)–Cu	78.8(1) × 2
Hf(2)–Se(4)–Cu	75.2(1) × 2
Cu–Se(4)–Cu	101.3(1)

Table 5
Evaluation of the Guinier diffraction diagram of $Tl_2Cu_2Zr_3S_8$

h	k	l	J	I_{obs}	$2\theta_{calc}$	$2\theta_{calc}$
0	0	1	2	422.1	6.96	6.85
2	0	−1	2	36.5	12.68	12.65
0	0	2	2	495.6	13.96	13.90
2	0	−2	2	172.0	15.14	15.10
2	0	1	2	179.8	17.84	17.80
2	0	−3	2	477.2	19.91	19.93
0	0	3	2	77.2	21.00	21.00
2	0	2	2	429.8	23.37	23.38
1	1	0	4	136.4	25.02	25.03
1	1	−1	4	132.1	25.22	25.25
4	0	−2	2	298.6	25.52	25.55
4	0	−1	2	256.1	25.72	25.77
1	1	1	4	173.2	26.77	26.77
1	1	−2	4	180.6	27.32	27.31
1	1	2	4	162.2	30.14	30.10
4	0	−4	2	135.7	30.55	30.52
3	1	−1	4	95.5	30.82	30.79
1	1	−3	4	102.3	30.96	30.92
3	1	−2	4	468.8	31.30	31.24
4	0	1	2	117.3	31.40	31.31
3	1	0	4	1000.0	31.96	31.91
2	0	−5	2	77.5	32.24	32.21
3	1	−3	4	483.5	33.35	33.30
1	1	3	4	117.1	34.72	34.70
0	0	5	2	628.8	35.36	35.32
1	1	−4	4	215.4	35.73	35.70
3	1	−4	4	110.5	36.74	36.67
3	1	2	4	354.1	38.43	38.40
6	0	−3	2	29.1	38.70	38.67
1	1	4	4	122.1	40.15	40.10
5	1	−2	4	121.5	40.30	40.27
4	0	−6	2	49.3	40.45	40.45
5	1	−3	4	77.7	40.94	40.92
3	1	−5	4	305.9	41.17	41.15
1	1	−5	4	42.6	41.30	41.25
4	0	3	2	70.9	41.65	41.55
6	0	0	2	237.6	42.24	42.23
6	0	−5	2	221.1	42.83	42.80
5	1	0	4	116.9	42.86	42.80
3	1	3	4	63.3	43.22	43.20
5	1	−5	4	150.7	45.85	45.85
5	1	1	4	42.1	45.89	45.85
1	1	5	4	64.7	46.21	46.21
4	0	−7	2	104.1	46.47	46.51
4	0	4	2	98.3	47.79	47.80
3	1	4	4	41.5	48.75	48.78
0	2	0	2	318.3	49.20	49.20
0	2	1	4	6.1	49.76	49.80
5	1	2	4	24.3	49.88	49.90
0	0	7	2	42.8	50.33	50.33
2	0	6	2	10.2	50.62	50.67
0	2	2	4	29.4	51.40	51.40
7	1	−3	4	21.9	51.84	51.87
8	0	−3	2	118.1	52.12	52.17
7	1	−2	4	78.8	52.17	52.17
3	1	−7	4	146.2	52.33	52.29
7	1	−4	4	86.1	52.58	52.64
2	2	1	4	18.7	52.75	52.74
1	1	6	4	8.7	52.77	52.74
7	1	−1	4	53.2	53.56	53.59
2	2	−3	4	63.6	53.58	53.59
2	0	−8	2	12.4	53.59	53.59
8	0	−5	2	13.1	53.80	53.79
0	2	3	4	9.2	54.05	54.09
1	1	−7	4	15.0	54.13	54.09
7	1	−5	4	42.0	54.37	54.41
4	0	5	2	4.9	54.43	54.41
3	1	5	4	196.5	54.89	54.88
2	2	2	4	80.1	55.15	55.18
7	1	−6	4	24.0	57.12	57.17
4	2	−3	4	6.4	57.14	57.17
2	0	7	2	29.1	58.22	58.21
3	1	−8	4	84.7	58.79	58.78
4	2	−4	4	33.8	59.03	59.03
7	1	1	4	100.9	59.26	59.25
1	1	7	4	39.9	59.79	59.83
7	1	−7	4	98.4	60.77	60.84
2	0	−9	2	26.9	61.32	61.28
0	2	5	4	238.7	62.03	62.02
4	2	2	4	7.2	62.54	62.49
7	1	2	4	20.8	63.41	63.44
8	0	−8	2	36.3	63.58	63.63
8	0	2	2	48.9	65.53	65.54
4	2	3	4	35.2	66.38	66.38
6	2	0	4	125.1	66.81	66.78
6	2	−5	4	119.6	67.24	67.20
6	0	5	2	44.3	67.77	67.77
9	1	−1	4	7.8	67.97	67.92
4	2	−7	4	63.8	69.99	70.00
9	1	−7	4	29.2	70.10	70.00
10	0	−7	2	49.8	70.64	70.64
4	2	4	4	61.7	71.02	71.02
0	2	7	4	28.7	73.03	73.05
5	1	−10	4	43.0	73.08	73.05
3	1	−10	4	32.8	73.26	73.23
7	1	4	4	23.4	73.97	74.03
8	2	−3	4	91.6	74.49	74.53
0	0	10	2	33.5	74.81	74.88
1	1	9	4	36.4	75.22	75.28
8	2	−6	4	16.0	77.86	77.88
11	1	−3	4	40.7	80.24	
7	1	5	4	26.8	80.31	80.33
1	3	−3	4	7.7	80.54	80.59

Space group $C2/m$, $a = 14.033(2)$ Å, $b = 3.7008(6)$ Å, $c = 13.874(3)$ Å, $\beta = 113.93(1)°$.

bicapped trigonal prismatic chalcogen coordination (Fig. 3). One of the rectangular faces of the trigonal prism uniquely shares its edges with two $CuSe_4$ tetrahedra and two $HfSe_6$ octahedra of the same anionic layer. By sharing common basal faces the trigonal prisms form infinite columns which are, in an antiparallel orientation, arranged in pairs (Fig. 4). Neighboring columns are shifted with respect to each other by $b/2$, thus providing one waist contact of the $TlSe_6$ prism ($d_{Tl-Se(3)} = 3.540(2)$ Å), while the other is formed to an additional chalcogen atom (Se(1)) at a distance comparable with those in the trigonal prisms ($d_{Tl-Se(1)} = 3.352(2)$ Å) (Table 4). Whereas the arrangement of the trigonal prisms in the $KCuZrS_3$ [1] structure type finds, as was shown recently [3], an antitype correspondence to the structure of Re_3B, the

Table 6
Evaluation of the Guinier diffraction diagram of $Tl_2Cu_2Zr_3Se_8$

h	k	l	J	I_{calc}	$2\theta_{calc}$	$2\theta_{obs}$
0	0	1	2	200.3	6.70	6.63
2	0	−1	2	86.4	12.36	12.35
2	0	0	2	12.7	13.43	13.40
0	0	2	2	224.5	13.43	13.40
2	0	−2	2	87.6	14.69	14.68
2	0	1	2	79.5	17.28	17.28
2	0	−3	2	251.8	19.25	19.23
0	0	3	2	18.6	20.20	20.15
2	0	2	2	191.3	22.58	22.50
1	1	0	4	32.7	24.19	24.12
1	1	−1	4	69.9	24.38	24.32
4	0	−1	2	53.8	25.07	25.00
1	1	1	4	72.8	25.86	25.83
1	1	−2	4	48.1	26.38	26.38
4	0	0	2	37.4	27.04	26.99
2	0	3	2	73.8	28.58	28.52
4	0	−4	2	196.8	29.64	29.60
3	1	−1	4	211.5	29.87	29.85
3	1	−2	4	461.7	30.33	30.30
4	0	1	2	193.6	30.47	30.48
3	1	0	4	1000.0	30.96	30.95
3	1	−3	4	440.4	32.28	32.28
1	1	3	4	136.8	33.47	33.48
0	0	5	2	611.0	34.00	34.01
1	1	−4	4	202.4	34.43	34.46
3	1	−4	4	123.1	35.51	35.51
3	1	2	4	256.8	37.13	37.15
6	0	−3	2	18.3	37.68	37.60
1	1	4	4	85.1	38.66	38.68
5	1	−2	4	141.7	39.12	39.10
3	1	−5	4	211.5	39.74	39.75
4	0	3	2	40.9	40.25	40.27
6	0	0	2	194.7	41.06	41.05
5	1	0	4	108.5	41.56	41.60
6	0	−5	2	166.5	41.59	41.60
3	1	3	4	27.8	41.71	41.72
5	1	−5	4	144.7	44.39	44.46
5	1	1	4	78.6	44.44	44.46
4	0	−7	2	43.0	44.81	44.79
3	1	4	4	70.6	46.98	46.98
0	2	0	2	371.6	47.46	47.45
0	0	7	2	38.4	48.32	48.33
2	0	6	2	17.3	48.65	48.65
0	2	2	4	12.9	49.55	49.57
3	1	−7	4	151.1	50.37	50.34
8	0	−3	2	110.5	50.72	50.69
7	1	−4	4	64.0	51.05	51.04
2	2	−3	4	33.6	51.67	51.69
7	1	−1	4	26.8	51.98	52.01
5	1	−7	4	31.9	52.74	52.81
3	1	5	4	248.2	52.83	52.81
2	2	2	4	35.1	53.17	53.21
7	1	0	4	16.3	54.25	54.33
8	0	−6	2	43.0	54.53	54.53
3	1	−8	4	104.8	56.51	56.52
4	2	−4	4	57.6	56.96	57.00
7	1	1	4	127.6	57.39	57.42
2	2	−5	4	52.1	57.81	57.82
7	1	−7	4	90.7	58.78	58.79
6	0	4	2	30.7	59.15	59.21
3	1	6	4	12.4	59.17	59.21
0	2	5	4	240.7	59.66	59.66
6	0	−9	2	17.9	60.21	60.28
8	0	−8	2	26.3	61.53	61.53
6	2	−3	4	7.3	62.13	62.12
4	2	−6	4	7.1	63.10	63.09
2	0	8	2	16.9	63.43	63.42
4	2	3	4	20.1	63.94	63.96
6	2	0	4	105.4	64.52	64.51
6	2	−5	4	91.9	64.91	64.88
6	0	5	2	36.5	65.27	65.26
1	1	−9	4	40.1	65.93	65.93
3	1	7	4	38.5	65.97	65.93
2	0	−10	2	32.0	66.50	66.50
2	2	−7	4	21.6	67.00	67.00
4	2	−7	4	25.3	67.32	67.27
5	1	−10	4	36.3	70.17	70.15
6	2	2	4	27.4	70.31	70.30
2	2	6	4	12.5	70.32	70.30
0	0	10	2	18.9	71.56	71.53
8	2	−3	4	86.5	71.99	71.96

Space group $C2/m$, $a = 14.392(3)$ Å, $b = 3.828(1)$ Å, $c = 14.387(3)$ Å, $\beta = 113.69(2)°$.

present compounds have no counterpart in binaries with trigonal prismatic coordination.

The Tl–Se bond length averaged over all eight neighbors is 3.333 Å, in good agreement with the sum of the ionic radii [11], indicating predominantly ionic interactions. From this geometry a significant stereochemical activity of the lone pair of electrons on Tl^+ is improbable.

The distorted tetrahedral chalcogen coordination of the copper atoms is close to C_{2v} and virtually corresponds to those in $TlCuZrSe_3$ or $TlCuHfSe_3$. The selenium neighbors constituting the largest bond angle Se(2)–Cu–Se(3) belong to two different selenohafnate chains, while the smallest bond angle is found with the Se(4) atoms which form the common vertices. The mean Cu–Se bond distance $\bar{d} = 2.431$ Å is in excellent agreement with the values found in $TlCuZrSe_3$ or $TlCuHfSe_3$ ($\bar{d} = 2.430$ Å) [3].

The variance of the Hf–Se bond lengths is rather small. The hafnium atoms Hf(1) which occupy the centers of the trans-octahedral chains have, as in $TlCuHfSe_3$, six equidistant Se neighbors. A larger spread is naturally observed for the central atoms Hf(2) in the double chains, reflecting the different number of Hf neighbors of the individual selenium atoms (three for Se(1), two for Se(2) and Se(4) respectively). The mean bond lengths are close together ($\bar{d}_{Hf(1)-Se} = 2.673$ Å and $\bar{d}_{HF(2)-Se} = 2.669$ Å) and slightly but significantly shorter than that found in $TlCuHfSe_3$.

Owing to their close structural analogy, $TlCuHfSe_3$ and $Tl_2Cu_2Hf_3Se_8$ can be regarded as the first members of a (hypothetical) series of compounds, $Tl_2Cu_2T^{IV}_{1+n}Q_{4+2n}$ ($n = 1, 2, \ldots$), which would be formed by vertex-sharing octahedral chains of increasing widths ending in the CdI_2 structure type ($n = \infty$)

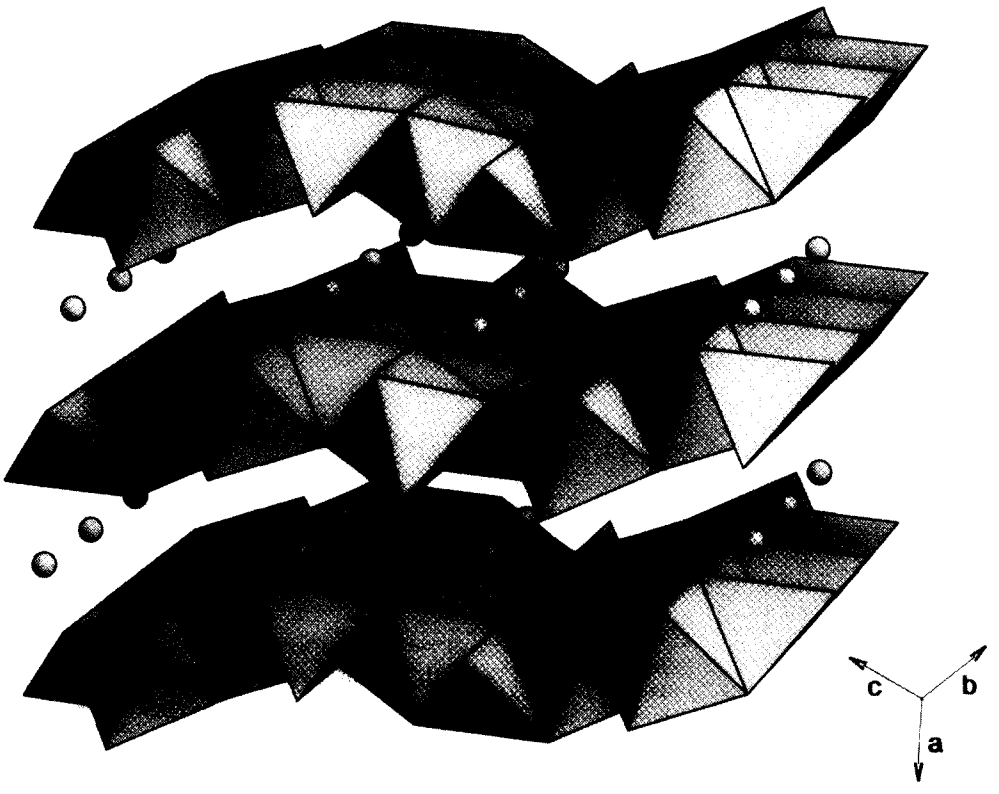

Fig. 1. Clinographic projection of the crystal structure of $Tl_2Cu_2Hf_3Se_8$. Dotted circles denote the Tl atoms, $CuSe_4$ tetrahedra and $HfSe_6$ octahedra in polyhedral representations.

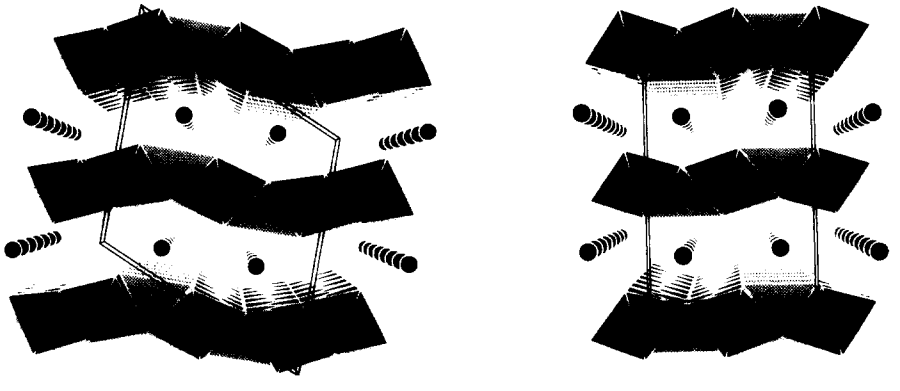

Fig. 2. Perspective views of the crystal structures of (a) $Tl_2Cu_2Hf_3Se_8$ along [010] and (b) $TlCuHfSe_3$ ($KCuZrS_3$-type [1]) along [100]. Thallium atoms are represented by filled circles.

which is realized in the dichalcogenides $T^{IV}Q_2$. Since the number of Tl and Cu atoms per formula unit remains fixed in this series, the formation of higher members involving triple or even more complex octahedral chains appears not very likely. However, a representative for $n = 3$, corresponding to $Tl_2Cu_2T^{IV}_4Q_{10}$, with layers built up by vertex-sharing of octahedral double chains might well exist and preparative efforts are currently in progress. Double octahedral chains as structural elements, first observed in $CuTaS_3$ [12,13], have since been found in a number of complex chalcogenides of the IVa metals, either as part of a three-dimensional framework, as in Cu_2HfTe_3 [14], Cu_2ZrTe_3 [14,15], Cu_2TiTe_3 [14,16] and $Cu_{2-x}Zr_{1+y}Se_3$ [17], or as isolated anionic moieties in $Tl_2T^{IV}Q_3$ (T = Zr, Hf; Q = S, Se) [18]. Layered anions incorporating this structural motif have been reported for $NaCuT^{IV}Q_3$ (T = Ti, Q = S; T = Zr, Q = Se, Te) [2]. In these compounds the double chains are connected via double rows of

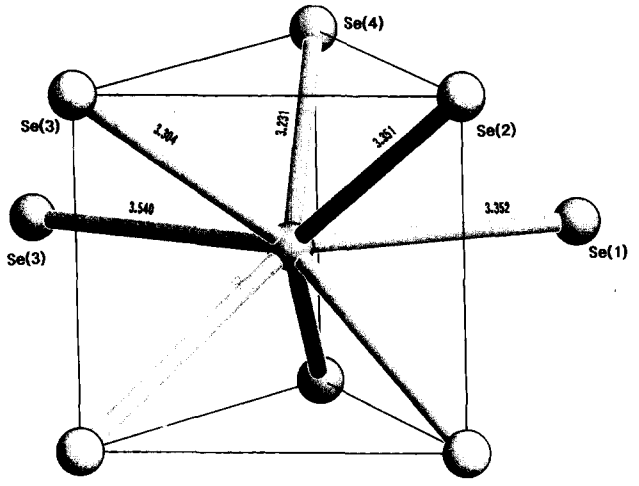

Fig. 3. The chalcogen coordination of the thallium atom in $Tl_2Cu_2Hf_3Se_8$.

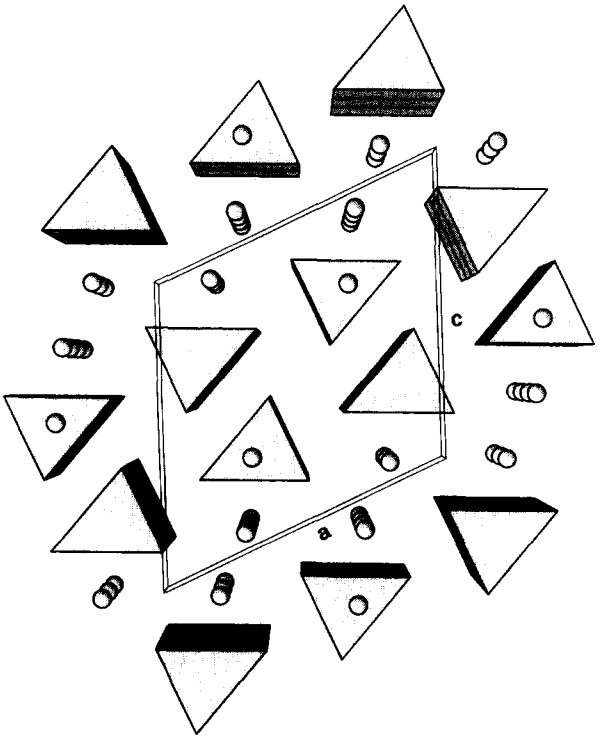

Fig. 4. The Tl–Se partial structure of $Tl_2Cu_2Hf_3Se_8$ showing the mutual arrangement of the columns of face-sharing $TlSe_6$ prisms. The trigonal prisms exert one waist contact to Se(1) (shown as dotted circles).

tetrahedrally coordinated copper atoms. A similar building principle is found in the novel thiozirconate $Na_2Cu_2ZrS_4$ [19], which though formally a member of the above mentioned series with $n = 0$ is characterized by layers of trans-octahedral single chains connected via copper atoms.

$Tl_2Cu_2Hf_3Se_8$ and its zirconium analogs are so far the only complex chalcogenides of the IVa metals where double and single octahedral chains coexist. Their formation offers a further example for structural diversity in this class of compounds.

References

[1] M.F. Mansuetto, P.M. Keane and J.A. Ibers, *J. Solid State Chem.*, *101* (1992) 257.
[2] M.F. Mansuetto, P.M. Keane and J.A. Ibers, *J. Solid State Chem.*, *105* (1993) 580.
[3] K.O. Klepp and D. Gurtner, *J. Alloys Comp.*, in press.
[4] E. Hovestreydt, *J. Appl. Crystallogr.*, *16* (1983) 651.
[5] F.A.S. Al-Alamy, A.A. Balchin and M. White, *J. Mater. Sci.*, *12* (1977) 2037.
[6] P. Main, S.J. Fiske, S. Hull, L. Lessinger, G. Germain, J.-P. Declercq and M.M. Woolfson, *Multan 11/88, A System of Computer Programs for the Automatic Solution of Crystal Structures from X-Ray Diffraction Data*, Universities of York, UK and Louvain, Belgium.
[7] *MolEN — An Interactive Structure Solution Procedure*, Enraf-Nonius Delft, Netherlands, 1990).
[8] D.T. Cromer and J.T. Waber, in J.A. Ibers and W.C. Hamilton (eds.), *International Tables for X-Ray Crystallography*, Vol. IV, Kynoch Press, Birmingham, UK, 1974, p. 72.
[9] D.T. Cromer, in J.A. Ibers and W.C. Hamilton (eds.), *International Tables for X-Ray Crystallography*, Vol. IV, Kynoch Press, Birmingham, UK, 1974, p. 149.
[10] N. Walker and D. Stuart, *Acta Crystallogr., A39* (1983) 158.
[11] L. Pauling, in *The Nature of the Chemical Bond*, Cornell University Press, Ithaca, NY, 1940.
[12] C. Crevecoeur and C. Romers, *Kon. Ned. Akad. Wet., 67B* (1964) 289.
[13] S.A. Sunshine and J.A. Ibers, *Acta Crystallogr., C43* (1987) 1019.
[14] P.M. Keane and J.A. Ibers, *J. Solid State Chem. 93* (1991) 291.
[15] K.O. Klepp and D. Mayr, *Z. Kristallogr., Suppl. 8* (1994) 624.
[16] W. Bensch, *Z. Kristallogr. 209* (1995) 687.
[17] K.O. Klepp and D. Gurtner, in preparation.
[18] K.O. Klepp and D. Mayr, *Proc. Eleventh Int. Conf. on Solid Compounds of Transition Elements*, Collected Abstracts, p. 57, Wroclaw, Poland, 1994.
[19] M.F. Mansuetto and J.A. Ibers, *J. Solid State Chem*, *117* (1995) 30.